

LA-8793-MS

Dr. 2609

R4151

**Evaluation of Savannah River Plant
Shuffler Calibration Standards**

University of California



LOS ALAMOS SCIENTIFIC LABORATORY

Post Office Box 1663 Los Alamos, New Mexico 87545

LA-8793-MS

UC-15

Issued: March 1981

Evaluation of Savannah River Plant Shuffler Calibration Standards

**M. M. Meier
T. W. Crane
C. J. Nachtsheim**

DISCLAIMER



EVALUATION OF SAVANNAH RIVER PLANT SHUFFLER CALIBRATION STANDARDS

by

M. M. Meier, T. W. Crane, and C. J. Nachtsheim

ABSTRACT

Six chemistry and three nondestructive assay (NDA) measurements have been made to provide information on the ^{235}U content of twelve standards cut from a cylinder of uranium-aluminum alloy to be used in calibrating the ^{252}Cf Shuffler. These data have been evaluated to produce a set of uranium mass estimates and associated uncertainties for the standards by means of least squares techniques. Longitudinal fluctuation in uranium density is modeled, both by linear splines and by polynomials, and the two methods are compared. Also, a method is given for assessing the accuracy of the measurement uncertainties initially provided.

I. INTRODUCTION AND SUMMARY

A ^{252}Cf Shuffler¹ has been installed at Savannah River Plant (SRP) to measure the ^{235}U content of waste and scrap generated at the reactor fuel fabrication facility. Measurements are performed by counting delayed neutrons from fission after an interrogating ^{252}Cf source is returned to a well-shielded position. Calibration standards are necessary to relate this neutron-counting response to the ^{235}U mass of the assay sample. It is the purpose of this report to describe the evaluation of such calibration standards.

A set of calibration standards was fabricated at SRP from an extruded, cylindrical ingot of uranium-aluminum alloy with a nominal mass ratio of 0.3:0.7. A section, roughly 40 cm long, was taken from the central, most uniform portion and was sliced to produce 14 disks 6 mm thick and 12 disks 25 mm thick. The disk diameters were 171 mm. Thin (6-mm) and thick (25-mm) disks were removed in alternating fashion from sequential positions on the

ingot, with thin disks taken from each end and adjacent thin disks taken from the center. Figure 1 illustrates the positioning of the disks. The thick disks were clad in aluminum with 1.3-mm wall thickness, and they serve as the calibration standards. After fabrication and cladding, each disk was weighed with a commercial scale to an accuracy of 0.1 g (0.006%). The thin disks were cut into quadrants, and two quadrants from each disk were destructively analyzed. The pair of quadrants chosen for analysis varied in a rotating fashion. This selection procedure is illustrated in Fig. 1. Three NDA measurements were taken from each thick disk, and four destructive analyses were performed on each thin disk (two from each quadrant). Section II describes the experimental procedures and the data.

The evaluation problem is to combine these nine data sets to produce a best set of ^{235}U mass values and associated uncertainties for the 12 calibration disks. The problem considered here is complicated by the fact that we did not assume that the experimental uncertainties provided were necessarily precise. Thus, in conjunction with the determination of calibration mass values and uncertainties, we give a method for adjusting measurement uncertainties so that they truly reflect variation in the measurement sets. Section III reviews this technique and other basic methodologies. Two approaches for obtaining calibration mass estimates, involving linear and polynomial interpolation, are presented in Sections IV and V, respectively; Sec VI compares the two methods. Although results showed few differences in terms of actual calibration disk mass estimates, we conclude that, in general, the polynomial methods considered lead to slight increases in both accuracy and precision.

II. EXPERIMENTAL PROCEDURES AND RESULTS

As mentioned in the introduction, a total of nine measurements that bear on the ^{235}U content of each disk have been performed. At SRP one set of quadrants has been analyzed for fractional uranium content by four different chemical techniques: potentiometric analysis, modified Davies-Gray titration (MDG), coulometric analysis, and isotope dilution mass spectrometry (IDMS).² A second set of quadrants was analyzed by the group at Los Alamos National Laboratory using a Los Alamos-automated spectrophotometer and isotope dilution mass spectrometry.³ The quadrant masses were determined at each laboratory by weighing. In addition, the isotopic distribution was done for each sample at Los Alamos.

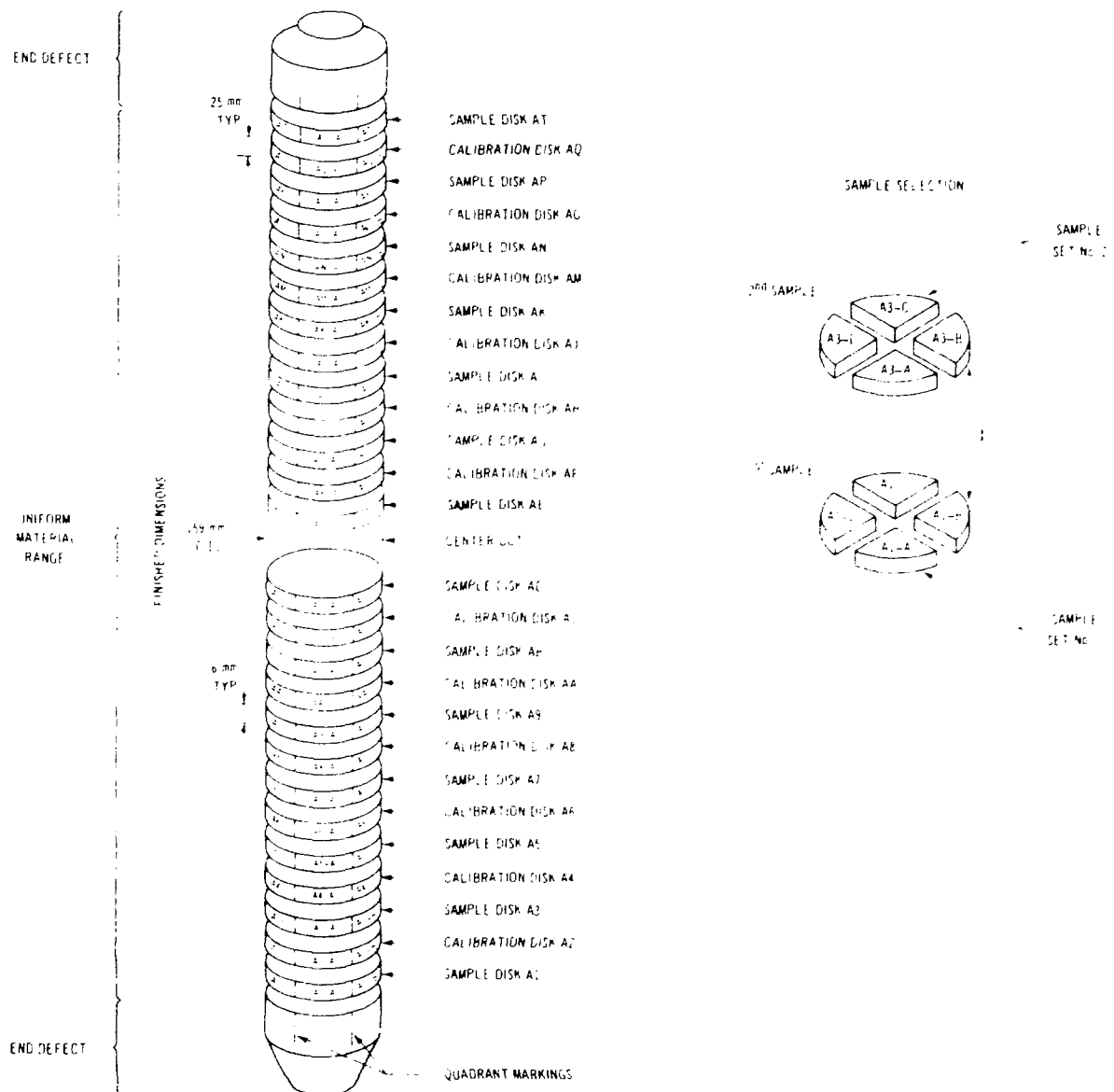


Fig. 1. Positioning of calibration and sample disks.

The Los Alamos chemistry measurements included the total mass, the uranium mass, and the uranium isotope distribution for each quadrant. Total mass uncertainty was less than 0.01% and was ignored. Uranium mass uncertainty was 0.19% and 0.26% for isotope dilution mass spectrometry and automated spectrophotometer, respectively. The ^{235}U fraction of total uranium had an uncertainty of 0.05%, which was ignored.

The SRP chemistry results were quoted in terms of uranium fractions that were converted to ^{235}U mass fraction by use of the Los Alamos isotopics data for each disk. The 0.05% uncertainties of the latter were again ignored. The uncertainties associated with the SRP chemistry results were: potentiometric analysis, 0.10%; modified Davies-Gray titration, 0.50%; coulometric analysis, 0.30%; and isotope dilution mass spectrometry, 0.30%.

At Los Alamos three other measurements were performed on the thick disks by nondestructive techniques. Reilly⁴ counted the 186-keV gamma rays from each disk and applied a transmission-dependent correction to account for attenuation in the sample. Reference 5 describes the counting of delayed neutrons after pulsed-neutron interrogation by the Van de Graaff accelerator. Finally, the Shuffler itself was used at SRP to produce a set of relative data for the 12 thick disks.

The Reilly gamma-ray spectroscopy data were the ^{235}U mass values for each of the 12 thick disks. These were combined with the SRP weighings of these disks to give the ^{235}U mass fraction. The total statistical uncertainty of this measurement was 0.46%, but observed nonuniformities in the samples introduce effects to which this method may be sensitive. Based on his measurements of variations in the transmission, Reilly estimates that systematic uncertainties may be as high as 3%. Because the nonuniformities were similar in character from disk to disk, we decided to assign the 0.46% uncertainty to the measurement and, if necessary, treat the data set as relative.

Van de Graaff data were quoted as ^{235}U mass, and the SRP weighings were used to convert them to ^{235}U mass fraction. These data have an uncertainty of 3%, the relative standard deviation of a standard analyzed concurrently with the disks. The ratios of Shuffler response to weighed mass for each thick disk comprise a final, relative set of data proportional to the ^{235}U mass fraction. The Shuffler response has uncertainties ranging from 0.08% to 0.11%.

Thus, the data to be analyzed consisted of 84 chemical and 36 NDA measurements and all associated uncertainties. For the linear interpolation analysis given in Sec. IV, three additional observations were made by interpolating each of the three pairs of NDA measurements from the adjacent thick disks. Table I gives the complete set of 120 observations, in addition to the interpolations and the weights used in the interpolations. Table I also provides uncertainty data. The relative standard deviations for each value were the same throughout each set except for the Shuffler data and are listed below

each data set. The range of Shuffler relative standard deviations is indicated, although in the evaluation procedure each measurement was associated with its specified uncertainty.

It must be emphasized that the relative standard deviations for sets 7 through 9 are for the measurement themselves, and not for the interpolated values used in the analyses. Standard deviations for the interpolated values were calculated using the identity

$$SD(a\mu_1 + b\mu_2) = \sqrt{[a \cdot SD(\mu_1)]^2 + [b \cdot SD(\mu_2)]^2}, \quad (1)$$

where SD represents standard deviation, μ_i is the i^{th} measurement, and a and b are the weights used in the interpolation. No interpolation error was incorporated in the assigned uncertainties.

III. BASIC ANALYSIS METHODOLOGY

The evaluation procedure uses the method of least squares as outlined in Ref. 6. The formalism will be briefly described here to show the modifications used in treating this problem and to define quantities that will have subsequent use.

Consider J masses each measured by A absolute techniques and R relative techniques. Information on the j^{th} mass can be obtained from the absolute measurements

$$M_j = \mu_{ij} \pm \sigma_{ij} \quad i = 1, 2, \dots, A, \quad (2)$$

and from the relative measurements

$$R_i M_j = \mu_{ij} \pm \sigma_{ij} \quad i = A + 1, A + 2, \dots, A + R. \quad (3)$$

Here (μ_{ij}, σ_{ij}) are the measurement values and associated uncertainties for the j^{th} mass measured by the i^{th} technique. Let M_j be the best value of the j^{th} mass to be determined by the evaluation and R_i be the best value of a factor that scales the i^{th} relative measurements to the absolute values.

TABLE I
235U MASS AND UNCERTAINTY DATA

Mass M _j	Set 1 LASL IDMS	Set 2 LASL Auto. Spect.	Set 3 SRP Potent.	Set 4 SRP MDG	Set 5 SRP Coulomb.	Set 6 SRP IDMS	Set 7 LASL VdG	Set 8 LASL γ Spect.	Set 9 LASL Shuffler
A1 Thick 1	16.46	16.46	16.56	16.45	16.46	16.47	17.32	15.91	2.475
A2 Thick 1									
A3 Thick 2	16.44	16.39	16.57	16.41	16.46	16.37	17.01 ^a	15.82 ^a	2.473 ^a
A4 Thick 2							16.76	15.72	2.471
A5 Thick 3	16.44	16.52	16.48	16.42	16.48	16.10	16.74 ^a	15.75 ^a	2.469 ^a
A6 Thick 3							16.79	15.78	2.467
A7 Thick 4	16.48	16.49	16.49	16.24	16.48	16.48	16.55 ^a	15.81 ^a	2.471 ^a
A8 Thick 4							16.32	15.84	2.474
A9 Thick 5	16.44	16.56	16.62	16.70	16.62	16.60	16.67 ^a	15.89 ^a	2.482 ^a
A10 Thick 5							17.02	15.91	2.484
A11 Thick 6	16.68	16.62	16.64	16.56	16.56	16.69	17.04 ^a	15.96 ^a	2.484 ^a
A12 Thick 6							17.07	16.00	2.483
A13 Thick 7	16.56	16.50	16.64	16.67	16.61	16.87	16.62 ^b	15.93 ^b	2.475 ^b
A14 Thick 7							16.45 ^b	15.90 ^b	2.472 ^b
A15 Thick 7	16.52	16.51	16.65 ^c	16.66	16.72	16.88	16.01	15.83	2.464
A16 Thick 9	16.46	16.44	16.54	16.39	16.61	16.74	16.43 ^a	15.78 ^a	2.461 ^a
A17 Thick 9							16.86	15.73	2.458
A18 Thick 10	16.58	16.53	16.41	16.33	16.44	16.79	16.54 ^a	15.85 ^a	2.461 ^a
A19 Thick 10							16.21	15.96	2.464
A20 Thick 11	16.43	16.47	16.48	16.34	16.53	16.42	16.62 ^a	15.90 ^a	2.464 ^a
A21 Thick 11							17.13	15.83	2.465
A22 Thick 11	16.52	16.51	16.40	17.45	16.46	16.40	17.16 ^a	15.87 ^a	2.466 ^a
A23 Thick 12	16.48	16.48	16.48	16.31	16.49	16.71	17.19	15.91	2.468
A24 Thick 12							16.62 ^a	15.89 ^a	2.468 ^a
A25 Thick 13	16.46	16.47	16.55	16.50	16.66	16.46	16.06	15.86	2.469
Estimated Standard Deviation × 10 ⁻³	2.6	1.6	5.6	3.0	3.6	30.0	4.6	9.7-11	

^aInterpolated: 1/2 (measurement of thick disk above) + 1/2 (measurement of thick disk below).

^bInterpolated: 7/12 (measurement of thick disk above) + 5/12 (measurement of thick disk below).

^cInterpolated: 9/12 (measurement of thick disk above) + 7/12 (measurement of thick disk below).

Because of the product term, $R_i M_j$, above, nonlinear least squares methodology is required to obtain best estimates M_j^0 and R_i^0 of the parameters M_j and R_i . Let M_j^0 be an estimate (for example, a weighted average of absolute measurements) of the best mass value for the j^{th} mass, and let R_i^0 be an estimate of the best scale factor for the i^{th} measurement technique. Then, using a Taylor expansion of the product term, normalized residuals for each measurement are

$$r_{ij} = \left[\frac{\Delta M_j}{M_j^0} - \frac{\Delta \mu_{ij}}{M_j^0} \right] \sigma_{ij}^{-1} \quad i = 1, 2, \dots, A \quad (4)$$

and

$$r_{ij} = \left[\frac{\Delta M_j}{M_j^0} + \frac{\Delta R_i}{R_i^0} - \frac{\Delta u_{ij}}{R_i^0 M_j^0} \right] \sigma_{ij}^{-1} \quad i = A+1, A+2, \dots, A+R \quad , \quad (5)$$

where

$$\Delta M_j = \hat{M}_j - M_j^0$$

$$\Delta R_i = \hat{R}_i - R_i^0$$

$$\Delta u_{ij} = u_{ij} - R_i^0 M_j^0$$

The best masses and scale factors are the values for which the sum of squares of residuals is minimized:

$$\frac{\partial}{\partial M_j} \sum_{i=1}^{A+R} \sum_{j=1}^J r_{ij}^2 = 0 \quad j' = 1, 2, \dots, J \quad , \quad (6)$$

$$\frac{\partial}{\partial R_i} \sum_{i=A+1}^{A+R} \sum_{j=1}^J r_{ij}^2 = 0 \quad i' = A+1, A+2, \dots, A+R \quad . \quad (7)$$

This gives rise to a set of $J + R$ equations linear in the J variables M_j and the R variables R_i that are amenable to solution by matrix inversion. For increased precision, solution variables \hat{M}_j and \hat{R}_i may be used as new sets of estimates M_j^0 and R_i^0 and the above process repeated until $\epsilon = \sum_j (M_j - M_j^0)^2 + \sum_i (R_i - R_i^0)^2$ is sufficiently small. (In general, for the data set under study, four iterations were sufficient to cause ϵ to drop below 10^{-10} .)

The best values, M_j and R_j , for the variables can then be explicitly reinserted into the expressions for r_{ij} , and the total weighted sum of squares computed:

$$\chi^2 = \sum_{i=1}^{A+R} \sum_{j=1}^J r_{ij}^2 \quad . \quad (8)$$

An overall estimate of variance is given by

$$B^2 = \chi^2 / [N - (J + R)] , \quad (9)$$

where N is the total number of data points and $N - (J + R)$ is the number of degrees of freedom. The standard deviation, B , is referred to as the generalized Birge ratio in Ref. 6. Taylor et al. (Ref. 6) define another parameter, b_i , which has a magnitude related to the compatibility of the i^{th} data set with the others evaluated.

$$b_i^2 = \left(\sum_{j=1}^J r_{ij}^2 \right) \left[n_i - \frac{n_i}{N} (J + R) \right]^{-1} , \quad (10)$$

where n_i is the number of data points in the i^{th} measurement set.

If all experimenters have assessed their uncertainties correctly, each of $B^2, b_1^2, \dots, b_{A+R}^2$ should be approximately 1. If this is not the case, the evaluator is confronted with the problem of modifying the input data or the results to produce best mass values and uncertainties consistent with the discrepant data. No well-defined procedures seem to exist for achievement of such conservative uncertainty estimates. The optimum solution, of course, would be to become intimately enough acquainted with the details of each experiment to be able to assess their uncertainties in an evenhanded fashion. Such a procedure would imply a level of acquaintance with the experiment at least equal to that of the experimenter. Even if possible, such a method would be extremely time-consuming and cumbersome.

Some evaluation procedures, notably those that generate best values for the fundamental constants,⁶ tend to favor inclusion of compatible data sets. Sets that are discrepant with the main body of data have a higher probability of rejection. As a result of this procedure, the best value of a fundamental constant may change by several standard deviations in a subsequent evaluation. (See, for example, Fig. 1, p. 7, Ref. 6.) Because further evaluations could not be expected, it was felt that a more conservative approach to the assignment of uncertainties was necessary.

Actually, if for some i , b_i^2 is much larger than 1, it indicates that the uncertainties associated with the i^{th} data set have been underestimated by a factor of b_i . Thus, a simple, compromise procedure is to multiply the

uncertainties associated with the i^{th} data set by the value Kb_i , where the constant, K , is chosen to give $B \approx 1$. In this way, as noted in Sec. I, the method chosen for adjusting uncertainties appropriately reflects uncertainty in the data.

Without detailing the mathematics, we note that in addition to best mass values, \hat{M}_j , the least squares analysis produces a $(J + R)$ by $(J + R)$ matrix Σ from which estimates of their variances and covariances are obtained. If the parameter estimates, $\hat{M}_1, \dots, \hat{M}_J, \hat{R}_1, \dots, \hat{R}_R$, are denoted P_1, \dots, P_{J+R} , then the $(i,j)^{\text{th}}$ entry of $C = B^2 \Sigma$ gives the estimated covariance of P_i and P_j . For $i = j$, C_{ii} is simply the estimated variance of P_i . The matrix C is needed, in particular, for determining standards uncertainties. For later reference, we note that the variance of any linear combination, $\sum_{i=1}^{J+R} a_i p_i$, of the parameters is given by

$$\text{Var} \left(\sum_{i=1}^{J+R} a_i p_i \right) = \sum_{i=1}^{J+R} \sum_{j=1}^{J+R} a_i C_{ij} a_j. \quad (11)$$

IV. A FIRST APPROACH: LINEAR INTERPOLATION

A. Method

Determination of best mass and uncertainty estimates for the calibration standards is accomplished in two steps. We first obtain uranium fraction and associated uncertainties for each of the 14 thin disks. Calibration disk masses are subsequently based on the simple linear interpolation or averaging of adjacent thin disk best mass values. Thin disk estimates are based on the 84 destructive analyses and the 36 interpolated NDA measurements. Because correlations in the data arise from interpolating thick disk values, generalized least squares procedures are required.

Briefly, the modification to the weighted least squares methodology already described is as follows. Let the unnormalized residuals, $r_{ij}' = r_{ij} \sigma_{ij}$, for the N observations be denoted e_1, \dots, e_N and let the covariance of e_i and e_j be given by ν_{ij} . The variance of e_i is ν_{ii} . Best masses are chosen to minimize $e' \nu^{-1} e$, where $e' = (e_1, \dots, e_n)$. In the foregoing, ν was simply a diagonal matrix with nonzero elements composed of the σ_{ij}^2 . Because correlations exist, ν is

no longer diagonal. For the generalized analysis, both an estimated variance, s^2 , and the square of the Birge ratio, B^2 , must be computed. This is necessary because B^2 now only approximates the estimated variance,

$$s^2 = \frac{\mathbf{e}' \mathbf{V}^{-1} \mathbf{e}}{[N - (J + R)]} . \quad (12)$$

Previously, it was possible to partition χ^2 into $A + R$ sums, $\chi_i^2 = \sum_j r_{ij}^2$, $i = 1, 2, \dots, A + R$. The expression b_i^2 was defined as $\chi_i^2 / \{n_i - (n_i/N)(J + R)\}$. For the generalized analysis, such a partitioning of $\mathbf{e}' \mathbf{V}^{-1} \mathbf{e}$ is not possible and, therefore, b_i^2 values computed will also be approximate.

B. Evaluation

The data of Table I were first inspected for consistency and biases. A calculation with all the data gave the results listed as Run A of Table II. The b_i^2 values indicate that sets 3, 4, 6 and 8 were the most discrepant. Examination of the residuals revealed that the 12th observation in Set 4 was somewhat aberrant. A T-test at the 0.01 level of significance rejected the case as an outlier. Deletion of the point led to an 87% reduction in the value of b_4^2 .

The large b_i value associated with data Set 8, the gamma spectroscopy measurement, was not wholly unanticipated. As mentioned in Sec. II, large systematic errors could have been introduced by the sample nonuniformities, although there is reason to suspect that they would act in the same way for all the samples. It was therefore decided to retain Set 8 unaltered but to use it as a relative data set and to delete the outlier of Set 4 for subsequent calculations. With these two changes the results labeled Run B were obtained. The value of R_8 was 0.9595, indicating a 4% bias in the Set 8 data.

Next, a series of calculations was done in which each absolute data set was permitted to be relative. This was done to seek out biases associated with any given measurement technique. Scale factors and values for B are listed under Run C for each absolute data set given relative status. Inspection indicates that there are no gross biases and that to account for the large value of B^2 one must assume that the uncertainties of one or more data sets are underestimated.

TABLE II
EVALUATION SUMMARIES FOR THE
LINEAR INTERPOLATION ANALYSES

Data set (i)	Run A	Run B	Run C		Run D	Run E	
	b_i^2	b_i^2	R_i	B^2	b_i^2	Scale Factor	b_i^2
1	2.57	3.88	0.9982	4.68	3.42	1.83	0.82
2	2.88	3.85	0.9967	4.56	3.96	1.95	0.86
3	9.54	6.40	1.0020	4.53	7.74	2.74	1.24
4	16.59	2.70	0.9951	4.66	- (deleted)	-	-
5	2.61	2.40	1.0007	4.81	2.73	1.63	0.76
6	17.46	16.97	1.0015	4.78	- (deleted)	-	-
7	0.87	0.77	1.0105	4.78	0.80	0.89	1.11
8	169.40	1.23			1.26	1.15	0.84
9	13.42	12.70			2.80	0.93	1.07
B^2	24.40	5.66			4.14		1.29
Variance (s^2)	14.97	4.98			1.56		1.17

At this point the SRP group was contacted and queried regarding the Set 4 outlier and large b_i value for Set 6. These results were apparently not surprising in view of the procedures followed for these two analyses. As a result of this discussion, it was agreed to omit Set 4 and Set 6 from subsequent evaluation. Run D of Table II gives the b_i values for the data base, excluding Sets 4 and 6.

Were the data not discrepant, as indicated by B^2 values significantly larger than 1, the evaluation would be complete, with the variance-covariance matrix specifying each mass uncertainty. Such is not the case, and the uncertainties for each data set must be adjusted using the procedure described in Sec. III. Each uncertainty for the i^{th} data set was multiplied by 0.985 b_i , and a reanalysis performed. The results are listed as Run E of Table II.

Table III lists mass values and relative uncertainties for each of Runs A through E as found by the generalized least squares analysis. The value of $\hat{\sigma}_i^2$ is given by the i^{th} diagonal element of the variance-covariance matrix, listed in Table IV, and estimates the variance of the i^{th} mass estimate, \hat{M}_i . The relative uncertainty is then $\hat{\sigma}_i/\hat{M}_i$. Notice that the

TABLE III
THIN DISK EVALUATED MASSES AND UNCERTAINTIES

Mass Number	Run A		Run B		Run D		Run E	
	Mass M_j (%)	$\sigma_j/M_j \times 10^{-2}$						
(j)								
1	16.47	0.30	16.47	0.17	16.48	0.15	16.47	0.1809
2	16.50	0.19	16.52	0.11	16.53	0.095	16.52	0.1218
3	16.47	0.17	16.49	0.10	16.50	0.086	16.49	0.1108
4	16.49	0.18	16.51	0.10	16.52	0.088	16.52	0.1127
5	16.57	0.18	16.59	0.10	16.59	0.091	16.58	0.1157
6	16.62	0.17	16.63	0.10	16.63	0.087	16.62	0.1117
7	16.59	0.16	16.61	0.090	16.60	0.078	16.58	0.0987
8	16.58	0.16	16.59	0.092	16.58	0.080	16.56	0.1005
9	16.50	0.18	16.51	0.10	16.50	0.088	16.48	0.1123
10	16.46	0.18	16.48	0.10	16.47	0.090	16.46	0.1153
11	16.45	0.19	16.74	0.11	16.47	0.094	16.47	0.1183
12	16.46	0.19	16.46	0.11	16.47	0.095	16.48	0.1200
13	16.47	0.19	16.49	0.11	16.49	0.095	16.49	0.1197
14	16.54	0.30	16.54	0.17	16.54	0.15	16.54	0.1809

sensitivity of the best mass values to the selected evaluation technique is quite low. The largest mass variation for all techniques is only $\pm 0.09\%$. Also, for runs of interest, B, D and E, uncertainty estimates are quite stable. However, it is felt that the use of the uncertainty scalings in Run E, as based on the discrepancy indicators b_j^2 in Run D, has resulted in more realistic assessments of uncertainties. As a result, the mass estimates $\{\hat{M}_j\}$ produced by Run E are the recommended set of best values.

The calibration disk masses, M_j^C and associated relative uncertainties, σ_j^C/M_j^C , $j = 1, \dots, 12$, as based on the results of Run E, are listed in Table V. The following formulae were used in their calculation.

$$M_j^C = \frac{1}{2}(\hat{M}_j + \hat{M}_{j+1}); \quad j = 1, \dots, 6. \quad (13)$$

$$M_j^C = \frac{1}{2}(\hat{M}_{j+1} + \hat{M}_{j+2}); \quad j = 7, \dots, 12. \quad (14)$$

The uncertainties were calculated using the variance-covariance matrix of the 14 best thin disk mass values (Table IV) and Eq. (1) of Sec. III. To facilitate calibration of the Shuffler at various levels of scrap mass and

TABLE IV
VARIANCE-COVARIANCE MATRIX OF THIN DISK MASS ESTIMATES^a

							j								
	1	2	3	4	5	6	7	8	9	10	11	12	13	14	
1	8.8786	0.0000	0.0000	0.0000	0.0000	0.0000	0.0000	0.0000	0.0000	0.0000	0.0000	0.0000	0.0000	0.0000	
2	0.0000	4.0466	1.5665	0.2094	0.3927	0.3366	0.2913	0.2748	0.3004	0.3957	0.3459	0.2518	0.4610	0.0000	
3	0.0000	1.5665	3.3366	1.3849	0.0734	0.3823	0.2544	0.2468	0.2796	0.3645	0.3175	0.2260	0.4265	0.0000	
4	0.0000	0.2094	1.3849	3.4636	1.6995	-0.0360	0.3268	0.2774	0.2454	0.3591	0.3071	0.2218	0.4125	0.0000	
5	0.0000	0.3927	0.0734	1.6995	3.6839	1.6619	-0.0585	0.0777	0.3209	0.2794	0.2685	0.1930	0.3510	0.0000	
i	6	0.0000	0.3366	0.3823	-0.0360	1.6619	3.4489	1.3951	0.7624	-0.1504	0.3957	0.2478	0.1974	0.3533	0.0000
7	0.0000	0.2913	0.2544	0.3268	-0.0585	1.3951	2.6840	2.4470	0.8458	0.0955	0.2502	0.1496	0.2974	0.0000	
8	0.0000	0.2748	0.2468	0.2774	0.0777	0.7624	2.4470	2.7767	1.4952	-0.0752	0.2707	0.1336	0.2835	0.0000	
9	0.0000	0.3004	0.2796	0.2454	0.3209	-0.1504	0.8458	1.4952	3.4320	1.6343	-0.0388	0.2477	0.2837	0.0000	
10	0.0000	0.3957	0.3645	0.3591	0.2794	0.3957	0.0955	-0.0752	1.6343	3.6012	1.3977	-0.1015	0.4911	0.0000	
11	0.0000	0.3459	0.3175	0.3071	0.2685	0.2478	0.2502	0.2707	-0.0388	1.3977	3.7995	1.7483	-0.0788	0.0000	
12	0.0000	0.2518	0.2260	0.2218	0.1930	0.1974	0.1496	0.1336	0.2477	-0.1015	1.7483	3.9106	1.6619	0.0000	
13	0.0000	0.4610	0.4265	0.4125	0.3510	0.3533	0.2974	0.2835	0.2837	0.4911	-0.0788	1.6619	3.8975	0.0000	
14	0.0000	0.0000	0.0000	0.0000	0.0000	0.0000	0.0000	0.0000	0.0000	0.0000	0.0000	0.0000	0.0000	8.9619	

^aThe (i,j)th entry gives the Cov (M_i, M_j). Cov (M_i, M_j) = Var (M_i). Each entry must be multiplied by 10⁻⁴.

TABLE V
LINEAR INTERPOLATION ANALYSIS (RUN E) CALIBRATION
DISK MASS AND UNCERTAINTY ESTIMATES

Disk	Total Mass (g)	Percentage Uranium	Mass Uranium (g)	Uncertainty (g)	Relative Uncertainty ($\times 10^{-3}$)
1	1671.13	16.494	275.64	0.30040	1.090
2	1680.62	16.501	277.32	0.27250	0.983
3	1666.62	16.496	274.92	0.25779	0.958
4	1646.30	16.546	272.39	0.26732	0.981
5	1675.13	16.606	278.18	0.27084	0.974
6	1674.66	16.613	278.21	0.25012	0.899
7	1664.47	16.537	275.25	0.25242	0.917
8	1673.58	16.479	275.78	0.26858	0.974
9	1678.23	16.467	276.35	0.26794	0.970
10	1674.02	16.472	275.74	0.28020	1.012
11	1675.35	16.480	276.11	0.27948	1.012
12	1672.86	16.517	276.31	0.29994	1.086

volume, Table VI lists best masses and uncertainties for combinations of 1 through 10 calibration disks. The particular combinations were chosen to keep the uncertainty associated with the total mass (approximately) as small as possible. Again, Eq. (1) was used to compute the listed uncertainties.

TABLE VI
LINEAR INTERPOLATION ANALYSIS (RUN E) MASS AND UNCERTAINTY
ESTIMATES FOR SELECTED COMBINATIONS OF CALIBRATION DISKS

Number of Disks	Combination	Mass Uranium (g)	Uncertainty (g)	Relative Uncertainty ($\times 10^{-3}$)
1	6	278.21	0.25012	0.899
2	6+7	553.45	0.42508	0.768
3	6+7+8	829.24	0.59983	0.723
4	5+6+7+8	1107.42	0.74130	0.669
5	5+6+7+8+9	1383.76	0.87726	0.634
6	4+5+6+7+8+9	1656.15	1.00489	0.607
7	4+5+6+7+8+9+10	1931.89	1.11906	0.579
8	3+4+5+6+7+8+9+10	2206.81	1.23202	0.558
9	3+4+5+6+7+8+9+10+11	2482.92	1.34767	0.543
10	2+3+4+5+6+7+8+9+10+11	2760.24	1.46084	0.529

C. Discussion

We note that other methods of interpolation might also have been suggested. For example, the thick disks, rather than the thin, could easily have been chosen as a basis for evaluation, resulting in a slightly different method of interpolation. In general, such a scheme will produce best mass estimates with increased variance; however, interpolation error may be reduced, especially if longitudinal variation in ^{235}U content is pronounced. Thus, in view of the method adopted, any evidence of strong longitudinal fluctuation in ^{235}U content might be cause for concern. Figure 2 shows the mass values of Run E plotted as a function of their initial positions along the ingot. The nonuniformity is large relative to the variances that result from the evaluation and suggests that the method chosen may have been inappropriate. In the case of the smooth and substantial longitudinal fluctuation in uranium content, regression procedures for estimating ^{235}U fraction as a polynomial function of position along the ingot may be most appropriate. Thick disk uranium content would then be obtained by integrating (averaging) the estimated

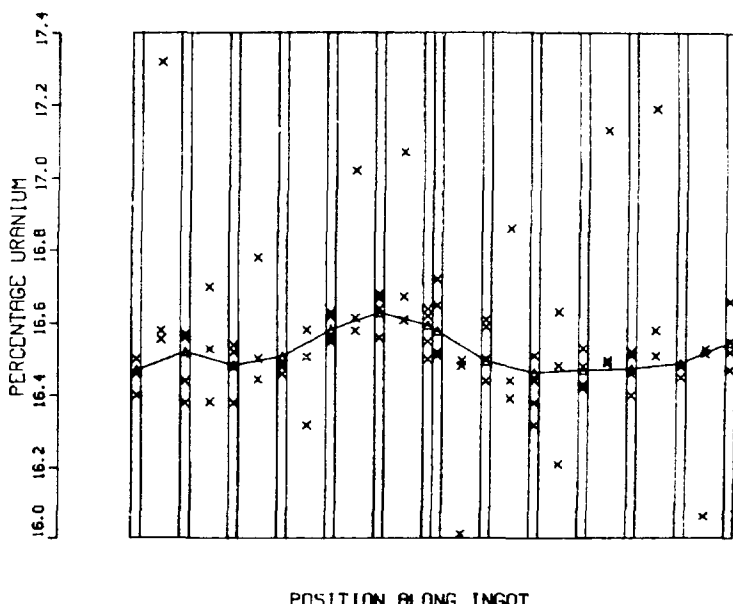


Fig. 2. Run E thin disk mass values plotted against position along ingot (Δ = mass estimate; x = measurement).

polynomial over the corresponding subregions of the rod. We consider this approach in detail in the next section.

V. A SECOND APPROACH: POLYNOMIAL INTERPOLATION

A. Method

In the previous section, evidence for significant longitudinal fluctuation in uranium content was found. Whereas no true physical model can be given to predict changes in uranium density, it was conjectured that polynomials may be useful in describing them. In this section we consider the estimation of uranium fraction as an i^{th} degree polynomial function, $p_i(x)$, of position x along the ingot. Given the least squares estimate, $\hat{p}_i(x)$, of the polynomial, calibration mass values are found by integrating $p_i(x)$ over the appropriate subregions of the log.

Briefly, the required least squares methodology is as follows. We assume that each observation $y_j(x_j)$, taken at log coordinate x_j , may be written

$$\begin{aligned} y_j(x_j) &= p_j(x_j) + e_j \\ &= \beta_0 + \beta_1 x_j + \beta_2 x_j^2 + \dots + \beta_i x_j^i + e_j . \end{aligned} \quad (15)$$

Let $\beta' = (\beta_0, \dots, \beta_i)$, $x' = (1, x_1, x_2^2, \dots, x_n^i)$, $x' = (x_1, \dots, x_n)$, $y' = [y_1(x_1), \dots, y_n(x_n)]$ and $e' = (e_1, \dots, e_n)$. Note that for the present analyses, none of the measurements, $y_j(x_j)$, are interpolated. Thus, the covariance of $y_j(x_j)$ and $y_k(x_k)$ is zero for $i \neq k$, and the variance-covariance matrix, V , of the data is diagonal with $V_{jj} = \text{Var}[y_j(x_j)] = \sigma_j^2$. For a specified degree i , the least squares coefficients, β_0, \dots, β_i , are chosen to minimize

$$s^2 = \hat{e}' V^{-1} \hat{e} / [N - (i + 1)] \quad (16)$$

and are given by

$$\hat{\beta} = (\hat{x}' \hat{V}^{-1} \hat{x})^{-1} \hat{x}' \hat{V}^{-1} \hat{y} . \quad (17)$$

The variance-covariance matrix of the estimated parameters is, in this case,

$$C = (X'V^{-1}X)^{-1}s^2. \quad (18)$$

Selection of a best order, i , for the model is accomplished by standard regression procedures and appropriate statistical tests (for example, examination of all possible regressions, residual plots, and the use of the F , R^2 , adjusted R^2 and C_p statistics; see Refs. 7 and 8 for further discussion.)

Given $p_i(x)$, best calibration disk mass estimates and uncertainties are obtained simply. For example, assume that the j^{th} calibration disk is bounded by log coordinates a_j and a_{j+1} . Then the estimated uranium percentage, f_j , for the j^{th} disk is given by

$$\begin{aligned} f_j &= \int_{a_j}^{a_{j+1}} \hat{p}_i(x) dx / (a_{j+1} - a_j) \\ &= \left[\hat{\beta}_0 x + \dots + \hat{\beta}_i x^{i+1} / (i+1) \right]_{a_j}^{a_{j+1}} / (a_{j+1} - a_j) \\ &= \sum_{k=1}^{i+1} \alpha_{j,k} \hat{\beta}_{k-1}, \end{aligned} \quad (19)$$

where

$$\alpha_{j,k} = (a_{j+1}^k - a_j^k) / (a_{j+1} - a_j).$$

From Eq. (11),

$$\text{Var}(f_j) = \sum_{k=1}^{i+1} \sum_{l=1}^{i+1} \alpha_{j,l} C_{l,k} \alpha_{j,k}. \quad (20)$$

Let m_j denote the total mass of the j^{th} calibration disk. Then $m_j f_j / 100$ is the uranium content and $m_j \sigma_j$ is the associated uncertainty, where the relative uncertainty, σ_j is given by

$$\sigma_j = \frac{\sqrt{\text{Var}(f_j)}}{100} . \quad (21)$$

B. Evaluation

Before the regression analysis could begin, we had to determine how to handle the relative data sets, 8 and 9. (Sets 4 and 6 were deleted as in the previous section.) Rather than attempt a nonlinear analysis such as described in Sec. III, we adopted a simpler two-stage approach: Initially, we used only the absolute data sets 1, 2, 3, and 5 to estimate the polynomial $p_i(x)$. From it we determined the average percentage, p , over the entire rod. We also computed simple weighted averages, w_8 and w_9 , of the eighth and ninth data sets. Appropriate scale factors were then given by $R_8 = w_8/p = 0.9596$ and $R_9 = w_9/p = 0.1495$. (Note that these values are extremely close to those found by the linear interpolation analysis, in which the R_8 and R_9 estimates were 0.9599 and 0.1496, respectively.) After scaling Sets 8 and 9 by R_8^{-1} and R_9^{-1} , respectively, we could treat all measurements as absolute. In the regression analyses that follow, x_j coordinates range from 0 to 3.72 (mm/100), and measurements $y_j(x_j)$ are percentage uranium.

An excellent fit to the data was given by a 7th-degree polynomial. We used the computed Birge ratios as presented in Table VII, Regression A, to adjust the measurement uncertainties as described in Sec. III and carried out a new analysis, regression B. Again, a polynomial of degree 7 was appropriate. The new Birge ratios are presented in Table VII. For comparision, the Birge ratios of the final linear interpolation analysis are also given. Although found by completely different techniques, the two sets of Birge ratios are strikingly similar.

Tables VIII and IX summarize the results of Regression B. Figure 2 illustrates the fitted polynomial and the data from which it was estimated. In addition to the least squares coefficients, Table VIII presents best mass and uncertainty values for each of the calibration disks. Best masses and uncertainties for those combinations of thick disks specified in Sec. IV are given in Table IX. (Table X presents the variance-covariance matrix of the parameters, used with Eq. (11) to compute the above uncertainties.)

TABLE VII
BIRGE RATIOS FOR REGRESSION ANALYSES
ON DATA SETS 1, 2, 3, 5, 7, 8, and 9
AND LINEAR INTERPOLATION ANALYSIS RUN E

Data Set (i)	Regression A b_i^2	Regression B b_i^2	Run E b_i^2
1	3.19	0.89	0.83
2	3.68	0.92	0.86
3	6.58	1.32	1.34
5	2.22	1.01	1.06
7	0.97	0.99	1.00
8	1.26	0.91	0.84
9	4.51	0.78	1.06
B^2	3.27	0.98	1.00
s^2	3.27	0.98	0.97

Comparison with the results of the linear interpolation analysis (Table VI) shows that the two methods yield uranium mass estimates for the various combinations that are extremely close. The largest difference occurs when all 10 calibration disks are included and is only 0.66g (2760.24g vs 2760.90g). The uncertainties produced by the polynomial analysis are generally less than 80% of those associated with the linear analysis. The question thus arises as to which set of results should be used. We consider this question in detail in the following section.

VI. A COMPARISON OF THE LINEAR AND POLYNOMIAL APPROACHES

Each of the methods described in the previous two sections can be criticized on separate grounds. The linear interpolation scheme, for example, may tend to underestimate longitudinal fluctuation, as noted previously. In contrast, with the polynomial approach, the possibility of overestimating variation in uranium density must be considered. As an extreme example, a 25th-degree polynomial could, of course, be constructed to intersect the weighted averages of the observations at each of the 26 (14 thin- and 12 thick-disk) points of support along the ingot. Clearly, the sinusoidal character of such a polynomial would very likely cause the interpolated estimates of thick disk uranium content to be significantly in error.

TABLE VIII
REGRESSION B^a CALIBRATION DISK MASS AND UNCERTAINTY ESTIMATES

Disk	Total Mass (g)	Percentage Uranium	Mass Uranium (g)	Uncertainty (g)	Relative Uncertainty ($\times 10^{-3}$)
1	1671.13	16.539	276.40	0.29208	1.057
2	1680.62	16.503	277.35	0.23928	0.863
3	1666.62	16.491	274.84	0.22515	0.819
4	1646.30	16.556	272.56	0.20851	0.765
5	1675.13	16.619	278.38	0.21717	0.780
6	1674.66	16.618	278.29	0.20174	0.725
7	1664.47	16.542	275.34	0.20360	0.739
8	1673.58	16.477	275.76	0.21772	0.791
9	1678.23	16.459	276.21	0.21785	0.789
10	1674.02	16.479	275.86	0.25220	0.914
11	1675.35	16.492	276.30	0.25220	0.913
12	1672.86	16.503	276.06	0.26701	0.967

^a $\beta = (16.471, 1.0353, -4.3975, 6.9723, -5.1384, 1.9194, -0.35414, 0.025691)$.

TABLE IX
REGRESSION B MASS AND UNCERTAINTY ESTIMATES FOR
SELECTED COMBINATIONS OF CALIBRATION DISKS

Number of Disks	Combination	Mass Uranium (g)	Uncertainty (g)	Relative Uncertainty ($\times 10^{-3}$)
1	6	278.29	0.20174	0.725
2	6+7	553.63	0.35790	0.647
3	6+7+8	829.39	0.50238	0.606
4	5+6+7+8	1107.78	0.58913	0.532
5	5+6+7+8+9	1383.99	0.67445	0.487
6	4+5+6+7+8+9	1656.55	0.74722	0.451
7	4+5+6+7+8+9+10	1932.41	0.84151	0.436
8	3+4+5+6+7+8+9+10	2207.25	0.90680	0.411
9	3+4+5+6+7+8+9+10+11	2483.55	0.97838	0.394
10	2+3+4+5+6+7+8+9+10+11	2760.90	1.02622	0.372

TABLE X
VARIANCE-COVARIANCE MATRIX OF ESTIMATED PARAMETERS OF REGRESSION B^a

	1	2	3	4	5	6	7	8
1	5.5727	35.0921	78.7776	85.7385	50.4214	16.3681	2.7577	0.1881
2	35.0921	1029.5000	3655.5900	5115.5600	3528.7700	1279.2300	233.6300	16.9475
3	78.7776	3655.5900	14283.0000	29935.9000	14876.8000	5505.1600	1020.9700	24.9274
4	85.7385	5115.5600	20935.9000	31555.5000	22858.6000	9580.1100	1608.44	16.2630
5	50.4214	3528.7700	14876.8000	22858.6000	16791.3000	6370.2800	1204.2100	89.7399
6	16.3681	1279.2300	5505.1600	8580.3100	6370.2800	2432.0300	463.8080	24.7566
7	2.7577	233.6300	1020.9700	1608.4400	1204.2100	463.8080	89.7628	6.6828
8	0.1881	16.9475	74.9274	119.0530	89.7399	34.7466	6.6828	0.5051

^aThe (i,j)th entry gives $\text{cov}(f_i, f_j)$. Each entry should be multiplied by 10^{-4} .

The following procedure was devised to gauge the relative accuracies of the two procedures. Thick disk uranium masses were first estimated by each of the methods without the use of the NDA (thick disk) measurements. Through the use of the PRESS (predicted residual sum of squares) statistic,⁸ we then determined which of the method could better predict the deleted calibration disk measurements. Let y_{ij} be the j^{th} measurement on the i^{th} calibration disk ($i = 1, \dots, 12$, $j = 1, 2, 3$) and let σ_{ij} be the uncertainty associated with y_{ij} . By f_i^L and f_i^P denote the estimated uranium percentages for the i^{th} calibration disk as determined by the linear and polynomial analyses, respectively. Then our procedure is to compare PRESS_L with PRESS_P where

$$\text{PRESS}_L = \sum_{i=1}^{12} \sum_{j=1}^3 \left[\frac{(f_i^L - y_{ij})}{\sigma_{ij}} \right]^2 \quad (22)$$

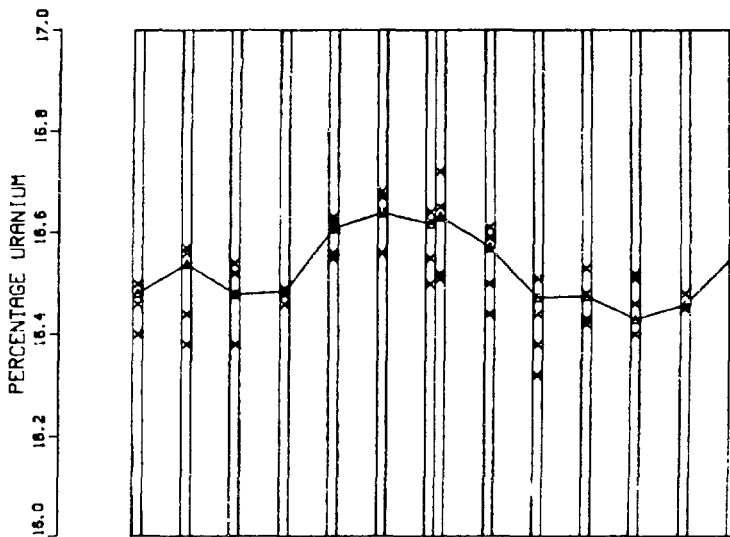
$$\text{PRESS}_P = \sum_{i=1}^{12} \sum_{j=1}^3 \left[\frac{(f_i^P - y_{ij})}{\sigma_{ij}} \right]^2. \quad (23)$$

Smaller PRESS values indicate better prediction efficiency.

The results of the linear and polynomial analyses are plotted in Figs. 3 and 4. In Fig. 3, best thin disk uranium percentage estimates, as determined by the linear analysis, are plotted and, to reflect the linear interpolations performed to obtain calibration disk estimates, are connected with straight lines. The fitted polynomial, again of degree 7, is plotted in Fig. 4. Note that the polynomial seems unstable at each end of the log. In particular, the lump centered over the left-most calibration disk appears to be unjustified and, at first glance, may mean that the polynomial is overestimating longitudinal flux in that region. Surprisingly, however, this is not the case. The NDA measurements taken from the left-most thick disk indicate that an increase in ^{235}U content, as predicted by the polynomial, does, in fact, occur (see Fig. 2). This leads to a reduction in PRESS_p relative to PRESS_l , and, as indicated by the computed values of the PRESS statistics ($\text{PRESS}_p = 0.00255$ and $\text{PRESS}_l = 0.00264$), overall, slight increases in accuracy may be attributed to the polynomial approach.

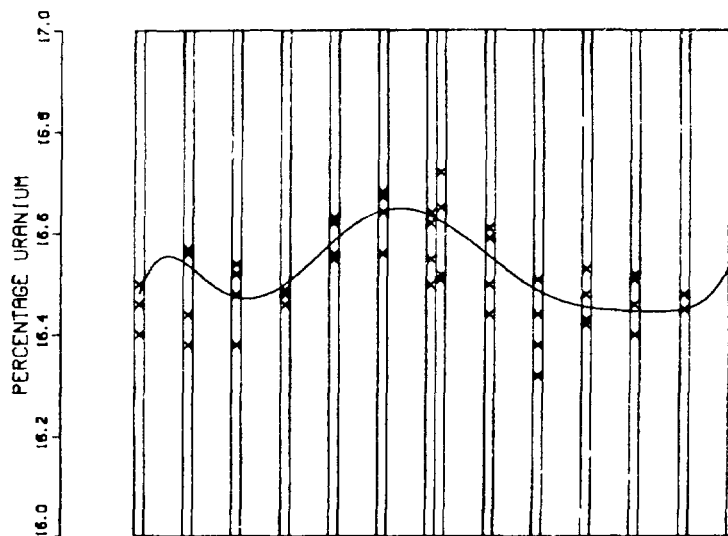
VII. CONCLUSIONS

Figure 5 illustrates the results of the linear and polynomial analyses. Thin disk uranium percentages, as determined by Run E in Sec. IV, are plotted and connected by straight lines. Superimposed on this linear spline is the seventh degree polynomial upon which the calibration disk mass estimates of Sec. V were based. The results show substantial agreements, especially for those calibration disks (2 through 11) to be used with the Shuffler. However, on the basis of the comparisons carried out in Sec. VI, the polynomial approach is preferred. Although slightly less conservative in terms of the uncertainty estimates provided, as indicated by the PRESS analysis of the preceding section, the method seems to more accurately characterize the longitudinal variation in ^{235}U density that occurs.



POSITION ALONG INGOT

Fig. 3. Best thin disk mass values plotted against position along ingot; linear analysis--NDA measurements excluded (Δ = mass estimate; x = measurement).



POSITION ALONG INGOT

Fig. 4. Polynomial estimate of percentage uranium content as a function of position along ingot; polynomial analysis--NDA measurements excluded (x = measurement).

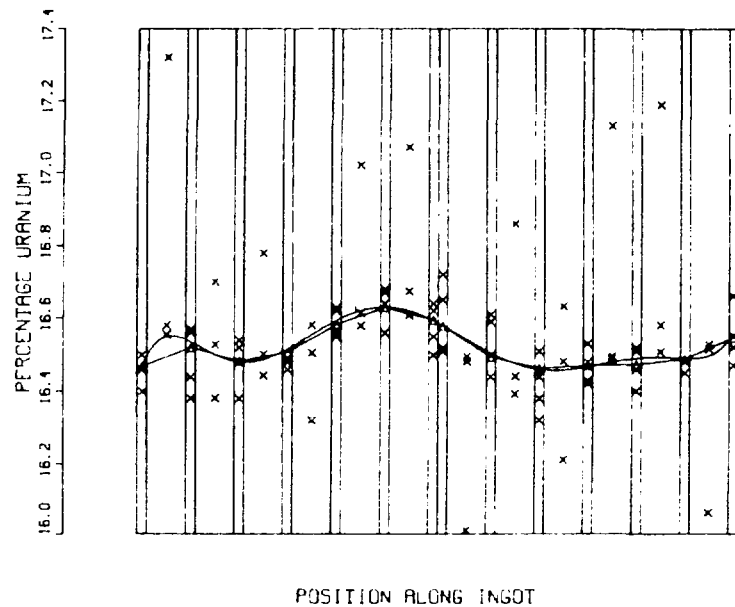


Fig. 5. Run E linear spline and Regression B polynomial estimates of uranium density vs position along ingot [Δ = best thin disk estimate from linear (spline) analysis; x = measurement].

ACKNOWLEDGMENTS

The authors would like to thank Dick Beckman of the Statistics Group at Los Alamos and Dennis Cook of the University of Minnesota for helpful suggestions.

REFERENCES

1. T. W. Crane, "Test and Evaluation Results of the ^{252}Cf Shuffler at the Savannah River Plant," Los Alamos National Laboratory unpublished data, 1980.
2. A. Gibbs and S. P. Boynton, "Uranium Standards for Californium Shuffler," E. I. du Pont de Nemours and Company, Savannah River Plant report DPSPU 78-11-19 (October 1978).
3. A. G. Sapanora, D. D. Jackson, S. F. Marsh, M. R. Betts, and D. J. Hoard, "Automated Spectrophotometer and Isotope Dilution Mass Spectrometry Analytical Results for the SRP Standards Material," Los Alamos National Laboratory, Analytical Chemistry Group report NB21643 (March 13, 1979).
4. T. D. Reilly, "Gamma Spectroscopic Examination of SRP Test Materials" (Q-1-78-731), Los Alamos National Laboratory memorandum to T. W. Crane (September 27, 1978).
5. "Standards for the SRP Shuffler" and "Gamma-Ray Measurements of SRP Shuffler Materials," in "Nuclear Safeguards Research and Development Program Status Report, September-December 1978," S. D. Gardner, Ed., Los Alamos National Laboratory report LA-7706-PR (May 1979), pp. 15-18.
6. B. N. Taylor, W. H. Parker, and D. N. Langenberg, The Fundamental Constants and Quantum Electrodynamics (Academic Press, New York, 1969).
7. N. R. Draper and H. Smith, Applied Regression Analysis (John Wiley and Sons, Inc., New York, 1966).
8. S. Weisberg, Multreg Users Manual (Department of Applied Statistics, University of Minnesota, St. Paul, 1980.)